Quantum Entanglement Based Computation of Energy Gaps for Open-shell Molecules

Lizbeth A. Lara[1]

[1]*School of Physical Sciences and Nanotechnology, Yachay Tech University, 100119-Urcuqui, Ecuador*

(Dated: June 20, 2024)

Quantum computers can efficiently perform full configuration interaction (FCI) calculations of atoms and molecules using the quantum phase estimation (QPE) algorithm. In the race to find efficient quantum algorithms to solve quantum chemistry problems, we will review the implementation of the Bayesian phase difference estimation (BPDE) algorithm. This method is employed to map wavefunctions for open-shell molecules and then calculates the difference between two eigenphases of unitary operator's energy gaps between two electronic states. The method is mainly based on the time evolution of the wave functions in the superposition of two electronic states, and the state preparation is carried out conditionally on the ancillary qubit. Thus, direct calculations of energy gaps are promising for future applications of quantum computers to solve fundamental chemistry problems.

1. INTRODUCTION

Currently, many specialists and industries consider that quantum computers have the potential to revolutionize several sectors, such as bio-medicine, cybersecurity, finance, and materials science. In addition to the diverse topics in quantum computing and quantum data processing, complex quantum chemical calculations referent to atoms and molecules are one of the most intensively studied fields as the future applicability of quantum computers [1]. Since the computational cost for full configuration (full-CI) calculations can provide the best possible wave functions within the space spanned by the basis, the set used increases exponentially concerning the size of the system [1]. However, as Feynman pointed out, quantum automatic systems can be efficiently simulated using a computer of quantum mechanical elements [7]. In this way, it precisely obeys quantum mechanical laws that utilize quantum mechanical principles such as superposition and entanglement of quantum states, that is, a quantum computer.

Note that if quantum computers (QCs) can perform complex and sophisticated quantum chemical computations of large and complex systems, it will help significantly in the road to understanding the chemical process in nature and the design of novel compounds and materials with valuable functionalities. For example, the first theoretical study of QPE-based full-CL was announced in 2005. In 2006, scientists at Waterloo and MIT succeeded in developing a 12-qubit system [2]. Also, several authors reported proof of principle experiments of the full-CI/STO-3G calculations of H_2 molecules by using photonic and **NMR** quantum computers in 2010 [3, 4]. Since then, many theoretical studies, including the quantum gate complexity enhancement [5–8], spatial and spin symmetry adaption [9–14], and experimental demonstrations of quantum chemical calculations, have been reported [15, 16]. Quantum computers can efficiently perform full configuration interaction (FCI) calculations of atoms and molecules using the quantum phase estimation (QPE) algorithm. However, QPE needs N qubits to read out the eigenphase in N binary digits. At the same time, interactive QPE (IQPE) and Bayesian phase estimation (BPE), relatives of QPE algorithms, use only one ancillary qubit [17, 18]. In the early attempts of the quantum FCI calculations, using Slater determinants to represent mapping wave function information as a linear combination onto quantum registers employing a direct mapping (DM) approach is common. In DM, each quantum bit (qubit) represents the one-to-one occupancy of a particular spin-orbital(i.e., $|1\rangle$ for being occupied and $|0\rangle$ for unoccupied)[10].

In 2014, Jeremy L. O'Brien et al. proposed a quantum-classical hybrid algorithm called a variational quantum eigensolver (VQE). It can compute the energy expectation values of approximated wave functions using currently available noisy intermediate-scale quantum (NISQ) devices. Furthermore, remarkable progress in quantum hardware is constantly being made. In 2019, IBM presented the Q-System, the first quantum computer. The company explained to newcomers that these computing paradigms were about a computer that could solve a series of more complex actions faster than conventional computers [19].

In addition, qubits were discussed as value units, leaving behind the traditional bits. Qubits, unlike bits, can take several values at once and perform computations that a conventional computer cannot do [19]. Besides, two-dimensional quantum walks on a 62-qubit system have been reported recently, and Google Inc. announced their aim for commercial-grade quantum computers by 2029 [20, 21]. In the QPE-based full-CI calculations, the time evolutions of the wave function $|\Psi\rangle$ using a Hamiltonian are simulated, and an energy eigenvalue E is extracted as a phase ϕ, as given in eqn (1), using inverse

quantum Fourier transformation.

$$e^{-iHt}|\Psi\rangle = e^{-iEt}|\Psi\rangle = e^{-i2\pi\phi}|\Psi\rangle \quad (1)$$

The computational cost of quantum chemical calculations on quantum computers increases significantly when we evaluate to finer digits. This increase is because QPE calculates the energy range where the full-CI solution is located rather than the full-CI energy itself [1]. In 2021, Takeji Takui and co-workers recently proposed a quantum algorithm, "Bayesian exchange coupling parameter calculator with broken symmetry wave functions (BXB)." It can directly compute the energy difference between two electronic states of different spin quantum numbers [22]. It can provide a prediction of the exchange coupling parameter J, which is half of the singlet-triplet energy gap, of small molecules within 1 $kcal\,mol^{-1}$ of precision, with a much lower computational cost than the convectional QPE-based approaches [1]. Regrettably, as discussed in detail in the next section, the BXB algorithm has drawbacks.

In this work, the results and methods of the last papers on the subject and, mainly, ones by Takeji Takui et al. are analyzed in order to 1) study the quantum algorithm that is capable of efficiently simulating the time evolution of wave functions [23]. 2) analyze how the information on the wave function is mapped and the preparation of a symmetry-adapted configuration state function $|\Psi_{\mathrm{CSF}}\rangle$, 3) present the quantum algorithm "Bayesian phase difference estimation (BPDE)" proposed by Takeji Takui. et al.. The BPDE capability is general in calculating the difference between two eigenphases of unitary operators and its application to direct calculations of various energy gaps. and its application to direct calculations of various energy gaps. Furthermore, numerical quantum circuit simulations for the direct calculations of vertical ionization energies of He, Li, Be, B, C, N, HF, BF, CF, CO, O2, NO, H2O, NH3, CH4, HCN, and HNC, singlet-triplet energy gaps of H2, C, O, NH, OH+, NF, NCN, and CNN, are reviewed.

Finally, the methodology and mathematical theory will be set in section 2, where we will discuss the functionality of the current different algorithms developed as solutions for chemical problems and their strengths and weaknesses compared to each other. Then, in section 3, we discuss and summarise the results of the main work [1]. Lastly, section 5 is dedicated to conclusions.

2. MATHEMATICAL METHODOLOGY

2.1 Definitions of quantum gates

In quantum computers, qubits can be an arbitrary superposition of the $|0\rangle$ and $|1\rangle$ states, as given in Eq.3. It means the representation of the superpositions of a qubit and the quantum states is given by:

$$|\psi\rangle = c_0|0\rangle + c_1|1\rangle \quad (2)$$

Where, c_0 and c_1 are arbitrary complex numbers satisfying the next normalisation condition Eq.3

$$|c_0|^2 + |c_1|^2 = 1 \quad (3)$$

Basis vectors can be expressed as orthonormal column vectors, called **kets** using the Dirac notation:

$$|0\rangle = \begin{pmatrix}1\\0\end{pmatrix} \qquad |1\rangle = \begin{pmatrix}0\\1\end{pmatrix} \quad (4)$$

Then, the quantum state $|\psi\rangle$ in Eq.2 can also be represented by a matrix as follows:

$$|\psi\rangle = \begin{pmatrix}c_0\\c_1\end{pmatrix} \quad (5)$$

A (2x2) unitary matrix can express quantum gates acting on one qubit, and the quantum state after the quantum gate application can be calculated using matrix algebra. For instance, the quantum state after the application of a Hadamard gate can be calculated by Eq.6

$$H_d|\psi\rangle = \frac{1}{\sqrt{2}}\begin{pmatrix}1 & 1\\1 & -1\end{pmatrix}\begin{pmatrix}c_0\\c_1\end{pmatrix} = \frac{1}{\sqrt{2}}\begin{pmatrix}c_0+c_1\\c_0-c_1\end{pmatrix} \quad (6)$$

Furthermore, it is necessary to define the Pauli matrices; these are a set of three 2×2 complex matrices which are Hermitian and unitary, denoted as:

$$\sigma_x = \begin{pmatrix}0 & 1\\1 & 0\end{pmatrix} \quad \sigma_y = \begin{pmatrix}o & -i\\i & 0\end{pmatrix} \quad \sigma_z = \begin{pmatrix}1 & 0\\0 & -1\end{pmatrix} \quad (7)$$

where we shall denote $Pauli-X$ for gate in the x-axis for σ_x and so on. It will help us in the construction of the wave function, and then it will be possible to map the wave function onto qubits. Moreover, it is necessary to define the Jordan–Wigner transformation (JWT). Since it will help map the wave function, this is defined as Eq 8:

$$a^\dagger = \sigma_r^+(\prod_{i<r}\sigma_i^2) \quad and \quad a_p = \sigma_p^-(\prod_{i<p}\sigma_i^2) \quad (8)$$

JWT is required to satisfy the Fermionic anticommutation relations of the operators because, in direct mapping DM, the information on the orbital occupancy of indistinguishable electrons is mapped onto distinguishable qubits. Then, the information on the wave function represented by a linear combination of Slater determinants is often mapped onto quantum registers through direct mapping (DM). Hence, the electronic Hamiltonian of a system is given by the second quantized formula with creation and annihilation operators, as given in Eq.9:

$$H = \sum_{p,q} h_{pq} {a_p}^\dagger a_q + \frac{1}{2}\sum_{p,q,r,s} h_{pqrs} a_p^\dagger a_q^\dagger a_r a_s \quad (9)$$

$$a_p^\dagger = \frac{1}{2}(X_p - i\,Y_p) \otimes \prod_{u=1}^{p-1} Z_u \tag{10}$$

$$a_p = \frac{1}{2}(X_p + i\,Y_p) \otimes \prod_{u=1}^{p-1} Z_u \tag{11}$$

$$H = \sum_m \mathcal{W}_m \mathcal{P}_m \tag{12}$$

Since the Hamiltonian in Eq.9 consists of noncommutative operators, using the Trotter-Suzuki decomposition is necessary to simulate the time evolution of the wave function. Great efforts have been made to carry out quantum FCI and related quantum chemistry problems using QCs [10]. For instance, using Bravyi-Kitaev transformation (BKT) instead of JWT, the number of controlled-NOT gates required for the Trotter decomposition may decrease significantly [10].

Then by applying Trotter-Suzuki decomposition, the time evolution operator $e^{(-iHt)}$ becomes in Pauli strings Eq.13

$$e^{-iHt} \approx \left| \prod_m e^{(-i\mathcal{W}_m \mathcal{P}_m t/N)} \right]^2 \tag{13}$$

In the next section, we summarise the Bayesian exchange coupling parameter calculator with the broken symmetry wave function (BXB) algorithm developed by Sugisaki et al. in [1, 24]. The BxB algorithm can directly compute the energy difference between two electronic states of different spin quantum numbers.

2.2 The BxB Algorithm

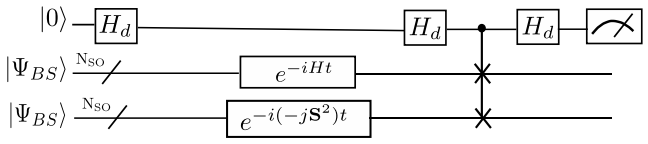

FIG. 1: A quantum circuit for the BxB algorithm. Adapted from [1].

Quantum superposition is one of the main quantum principles that utilize quantum computers as their computational resources, making it possible to directly compute the energy difference between two electronic states on QCs by utilizing the wave function approximated by a superposition of two electronic states. The BXB quantum algorithm reported by Sugisaki et al., in Fig.1 uses a broken-symmetry wave function $|\Psi_{\rm BS}\rangle$, a mixture of wave functions belonging to different spin quantum numbers. For the two-spin systems, $|\Psi_{\rm BS}\rangle$ is described as in Eq.14.

$$\begin{aligned} |\Psi_{\rm BS}\rangle &= |2\cdots 2\alpha\beta 0\cdots 0\rangle \\ &= \frac{1}{\sqrt{2}}(|\Psi_{S=1,M_s=0}\rangle + |\Psi_{S=0,M_s=0}\rangle) \end{aligned} \tag{14}$$

This wave function is used for the calculations of an exchange coupling parameter J However, the BXB algorithm has limitations. For example, it can compute the singlet-triplet excitation energy but not the singlet-singlet excitation energies because it uses the SWAP test. Therefore, the number of qubits required for implementation is approximately double that of the conventional QPE-based full-CI.

2.3 The BPE Algorithm

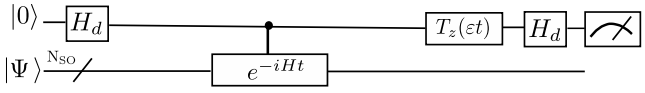

FIG. 2: A quantum circuit for the BPE algorithm. Adapted from [1].

The quantum circuit for BPE is illustrated in Fig.2. Here, horizontal lines specify a qubit or N_{SO}, representing the number of spin orbitals in the active space. An approximate wave function $|\Psi\rangle$ having a sufficiently large overlap with the full-CI wave function of the target electronic state is needed as the input for the BPE algorithm. The Hartree-Fock wave function $|\Psi_{\rm HF}\rangle$ is often used as $|\Psi\rangle$ for the ground state calculations of closed-shell singlet molecules. BPE starts by applying an Haddamard gate ($H_{\rm d}$) to the ancillary qubit at the top of Fig.2. The next step is for the controlled-time evolution of $|\Psi\rangle$. Furthermore, the time evolution operator is applied to $|\Psi\rangle$ if and only if the ancillary qubit is in the $|1\rangle$ state.

2.4 A Bayesian phase estimation (BPDE) algorithm

QPE algorithms, including IQPE and BPE, are challenging to implement on real quantum devices. The main reason is that the quantum circuit for the time evolution is extensive; thus, quantum error fixes are necessary to

obtain meaningful computational results. Another reason is that QPE needs a controlled time evolution operation. That operation requires many controlled-R_z gates with the same control qubit but different target qubits. Therefore, some quantum devices based on superconducting circuits can only execute two qubits gates between physically connected qubits [1]. In order to apply the controlled-R_z gate to two qubits that are not directly connected, one has to construct a SWAP network to exchange the quantum states of the neighboring qubits[1]. The SWAP networks require $O(N_{\mathrm{SO}})$ of additional gates, where is used a **big-Oh notation** to represent quantum gate complexity and N_{SO} is the number of the spin orbitals in the active space [1]. Therefore, even if all qubits are fully connected, one must minimize the crosstalk errors of the controlled-R_z gates. It would be helpful if QPE could be implemented without controlled-time evolution operations.

In addition, let us rethink the QPE algorithms mechanism. It computes the phase shift caused by the time evolution of wave functions and reads out the eigenphase by inverse quantum Fourier transformation (QPE) or Bayesian inference(BPE). Also, the controlled time evolution is introduced to calculate the phase difference of wave functions before and after the time evolution [22]. Nevertheless, it is possible to calculate the energy difference between two electronic states by simulating the time evolution of the wave function in the two electronic states, quantum simulation without controlled operations. Thus, if we can prepare the quantum superposition of the two electronic states conditional to the quantum state of the ancillary qubit, this represents the fundamental idea in the quantum algorithm for direct calculations of energy gaps [1, 25, 26].

Then, the quantum circuit for the BPDE algorithm is given in Fig.3; the quantum circuit reported from Osaka University research consists of one ancillary qubit and N_{SO} of qubits storing the wave function. Here, $|\Psi_0\rangle$ can be any approximated eigenfunction of Hamiltonian H. Unless otherwise specified, assume that $|\Psi_0\rangle$ is the approximated wave function of the electronic ground state. The quantum circuit starts with a Hadamard gate on the ancillary qubit to generate the superposition of the $|0\rangle$ and $|1\rangle$ states. Then, the following controlled-Excit gate denoted by c-Excit in Eq.15 applies an excitation operator to the wave function $|\Psi_0\rangle$ if and only if the ancillary qubit is in the $|1\rangle$ state. Thus, this operation generates the ground and excited states' superposition, as shown on the right-hand side of Eq.15. Then, subsequent time evolution operation and inverse-controlled-Excit operation transform the quantum state as Eq.16 and 17.

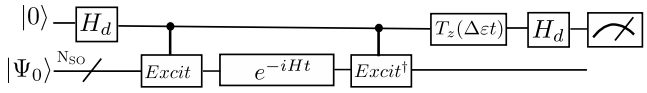

FIG. 3: A quantum circuit for the BPDE algorithm. Adapted from (Sugisaki, 2021).

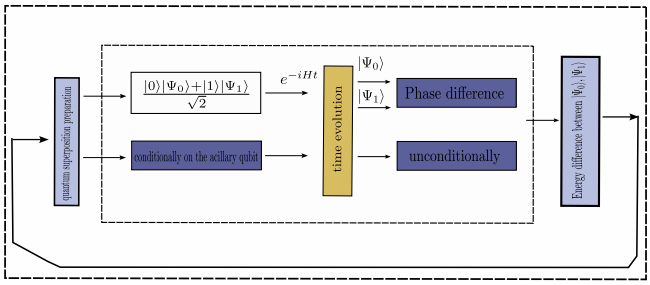

FIG. 4: Schematic representation for the BPDE algorithm. Adapted from (Sugisaki, 2021).

Fig.4 shows a schematic process representation for the BPDE algorithm. BPDE starts by preparing a superposition of two wave functions $|\Psi_0\rangle$ and $|\Psi_1\rangle$, which occurs conditionally on the ancillary qubit. The phase difference on the two wave functions is obtained after applying the time evolution operator $e(-iHt)$. After time evolution, this operation is unconditionally on the ancillary qubit. Finally, this returns the energy difference between the two wave functions.

$$\frac{1}{\sqrt{2}}(|0\rangle+|1\rangle)\otimes|\Psi_0\rangle \xrightarrow{c-Excit} \frac{1}{\sqrt{2}}(|0\rangle\otimes|\Psi_0\rangle+|1\rangle\otimes|\Psi_1\rangle) \tag{15}$$

$$\xrightarrow{exp(-iHt)} \frac{1}{\sqrt{2}}(|0\rangle\otimes e^{-iE_0t}|\Psi_0\rangle+|1\rangle\otimes e^{-iE_1t}|\Psi_1\rangle) \tag{16}$$

$$\xrightarrow{c-Excit^{\dagger}} \frac{1}{\sqrt{2}}(e^{-iE_0t}|0\rangle+e^{-iE_1t}|1\rangle)\otimes|\Psi_0\rangle \tag{17}$$

$$\xrightarrow{T_z(\Delta\varepsilon t)\otimes 1} \frac{1}{\sqrt{2}}(e^{-iE_0t}|0\rangle+e^{-i(E_1-\Delta\varepsilon)t}|1\rangle)\otimes|\Psi_0\rangle \tag{18}$$

$$\xrightarrow{H_d\otimes 1} \frac{1}{2}(e^{-iE_0t}+e^{-i(E_1-\Delta\varepsilon)t})|0\rangle\otimes|\Psi_0\rangle$$

$$+\frac{1}{2}(e^{-iE_0t}-e^{-i(E_1-\Delta\varepsilon)t})|1\rangle\otimes|\Psi_0\rangle \tag{19}$$

The next step to execute is the application of the phase shift gate T_z to the ancillary qubit, which gives the quantum state in Eq.23. Then, applying another Hadamard

gate on the ancillary qubit, the quantum state before the measurement in Fig 4 is given as the probability to obtain the $|0\rangle$ state in the measurement of the ancillary qubit, which is given by Eq.20:

$$P(0) = \frac{1}{2}[1 + \cos\{(E_1 - E_0 - \Delta\varepsilon)t\}] \qquad (20)$$

From Eq.25, it is easy to observe that the measurement of the ancillary qubit always gives the $|0\rangle$ state if $E_1 - E_0 = \Delta\varepsilon$. Hence, it is possible to compute the energy gap between the two electronic states by optimizing the phase shift angle $\Delta\varepsilon t$ through Bayesian inference implementation. Also, the BPDE algorithm does not need a penalty operator as others [1]. It can compute the difference between two eigenphases of unitary operators if one can conditionally generate the superposition of two eigenfunctions [1]. Moreover, it is necessary to emphasize that the BPDE algorithm application is not limited to quantum chemical calculations but a wide variety of eigenvalue problems.

The BPDE quantum algorithm has qualities that make it the best option to execute compared to the others. Qualities such as requiring only one ancillary qubit, which is the same in IQPE and BPE, provide the range for the possible value for $P(0)$, which is more expansive than in BxB. Thus, the $P(0)$ variation by changing $\Delta\varepsilon$ becomes more noticeable. Moreover, BPDE is free from controlled time evolution operations, whereas BPE and QPE require it. Another merit of the BPDE algorithm is that the controlled operations appear in the state preparation (controlled-Excit) and inverse state preparation ($controlled-Excit^{\dagger}$). The controlled excit generates the excited state wave function conditionally. Therefore, the quantum circuit for the controlled-excit has a depth similar to that used for the state preparation in traditional QPE-based approaches.

Furthermore, preparing the exact eigenfunction of a target electronic state in QPE is unnecessary, and preparation of the approximate wave function having sufficiently considerable overlap with the target electronic state is enough. Thus, the situation is the same in the BPDE algorithm. Correctly calculating the energy gap is possible if the controlled exit can conditionally generate the wave function overlapping with the target excited state. Finally, the quantum circuit for the controlled exit usually needs to be deeper. Thus, implementing BPDE is much easier than IQPE and BPE, which need controlled time evolution operations.

3. RESULTS AND DISCUSSION

3.1 Vertical ionization energies

Accurate calculations of ionization energies are important to understanding electron transfer and oxidation processes in chemical reactions and the nature of chemical bonding. Kenji Sugisaki et al. demonstrated in [27] that direct calculations of vertical ionization energies are possible by using the BxB algorithm. Here, we review how the BPDE algorithm is implemented to calculate the vertical ionization energies of CH4, HCN, and HNC molecules as well as 16 chemical species (He, Li, Be, B, C, N, HF, BF, CF, CO, O2, NO, CN, F2, H2O, and NH3) studied previously by using the BxB algorithm in [28]. To calculate the vertical ionization energies with the BPDE algorithm, they set the starting wave function $|\Psi_0\rangle$ to be $\mathrm{RHF/6-311G(d,p)}$ or the $\mathrm{ROHF/6-311G(d,p)}$ wave function for closed shell and open-shell species, respectively, of the neutral state. The largest systems under review are HCN and HNC with (10e, 9o) active spaces, those corresponding to 19 qubit quantum circuit simulations (18 qubits for the wave function storage and one ancillary qubit). Under the JWT, the controlled- Excit gate is realized by a CNOT gate with the ancillary qubit as the control and the qubit storing the occupation number of spin orbitals of which electron ionization occurs as the target. Kenji Sugisaki et al. used the ionization energy at the ΔSCF level, $\mathrm{IE(\Delta SCF) = E_{HF}(cation) - E_{HF}(neutral)}$, as the initial estimate of the vertical ionization energies.

The difference between the vertical ionization energies from the quantum circuit simulations and that one from the CAS-CI calculations are plotted in **Fig.5**, and the values of the BPDE, BPE, and CAS-CI ionization energies in conjunction with experimental ones are summarised in Table S2 in the ESI.† For all chemical species under study, the BPDE and BPE algorithms reproduced the CAS-CI ionization energy within 0.1 eV of errors. The ionization energies computed using BPDE and BPE are very close, revealing that the accuracy of the vertical ionization energy is almost the same between the direct calculation and naive approach. Both BPE and BPDE exhibit large deviations from the CAS-CI values in the HF molecule. The deviation can be rationally explained by the errors arising from Trotter decomposition. The deviation from the CAS-CI value systematically improves by increasing the number of Trotter slices, and it becomes 0.004 eV if we use five times larger the number of Trotter slices in the calculation of HF molecule [1].

The efficiency of the BPDE algorithm is evident in its convergence after just eight optimization cycles for all atoms and molecules under review. This system size independence feature is a significant advantage over the BPE method, where the number of Bayesian optimization cycles increases with the system size. For instance, the BPE optimization of the neutral and cationic states of F_2 required 11 iterations. This efficiency becomes

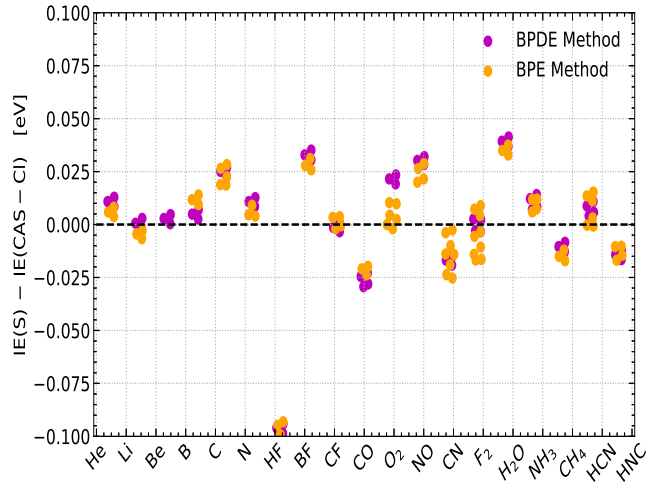

FIG. 5: Differences between the vertical ionization energies from the quantum circuit simulations and those from the CAS-CI calculations for chemical species under study. Adapted from [1].

even more crucial in the calculations of larger molecules and those containing heavier atoms, as demonstrated in the excitation energy calculations of CBr2 (see Section 3.3). The difference distribution between the vertical

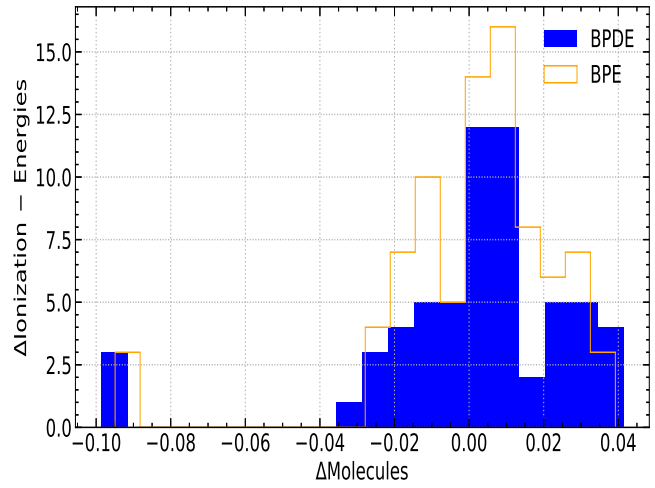

FIG. 6: Distribution for differences between the vertical ionization energies from the quantum circuit simulations and those from the CAS- CI. Adapted from (Sugisaki, 2021).

ionization energies from the quantum circuit simulations and that from the CAS-CI calculations can be observed in **Fig.6** which reveals that the BPDE result overlaps enough with the results of BPE. Besides, BPDE shows a high accuracy with the same number of qubits to be implemented as the BPE but with the advantage that it is easier to be implemented in QCs since the BPDE does not require any controlled time evolution operation that is one of the most difficult parts of quantum algorithms implementation to real quantum devices.

3.2 Singlet-triplet energy gaps

Another application of the BPDE algorithm is the direct calculations of singlet-triplet energy gap $\Delta E_{\text{S-T}}$ [1]. The singlet-triplet energy gap is the most important physical quantity in biradicals. The $\Delta E_{\text{S-T}}$ of biradicals are usually in the order of a few kcal mol^{-1} or less, and obtain accurate calculations of $\Delta E_{\text{S-T}}$ using quantum computers are very cost demanding. For the calculation of the singlet-triplet energy gap, the "$|\Psi_{\text{CSF}}\rangle$" of the $M_s = 0$ of the spin-triplet state given in Eq. 21 is implemented as $|\Psi_0\rangle$, and the spin-singlet state given by Eq. 22 is assigned to the excited state $|\Psi_1\rangle$. Indeed, $\Delta E_{\text{S-T}}$ becomes negative if the spin-singlet state has lower energy than the spin-triplet state.

$$|\Psi_{S=1,M_s=0}\rangle = \frac{1}{\sqrt{2}}(|2\ldots 2\alpha\beta 0\ldots 0\rangle + |2\ldots 2\beta\alpha 0\ldots 0\rangle) \tag{21}$$

$$|\Psi_{S=0,M_s=0}\rangle = \frac{1}{\sqrt{2}}(|2\ldots 2\alpha\beta 0\ldots 0\rangle - |2\ldots 2\beta\alpha 0\ldots 0\rangle) \tag{22}$$

By setting $|\Psi_0\rangle$ and $|\Psi_1\rangle$ as described above, the controlled-Excit operation becomes a controlled-Z gate with the ancillary qubit as the control and one of the qubits storing the occupation number of singly occupied molecular orbitals (SOMOs) as the target [1]. Then, the results for $\Delta E_{\text{S-T}}$ values calculated at the BPDE, BPE, and CAS-CI methods are shown below in **table I**. From Fig.7, both the BPE and BPDE succeed in predicting $\Delta E_{\text{S-T}}$ within 2 kcal mol^{-1} of errors in all systems. This corresponds to 1 kcal mol^{-1} of energy precision in the exchange coupling parameter J used in [27].

The results summarised in **table I** were obtained from the provided electronic supplementary data after the proper computation of the average for the five iterations of the singlet-triplet energy gap values executed in (Sugisaki, 2021). Departures of the $\Delta E_{\text{S-T}}$ (BPE) and $\Delta E_{\text{S-T}}$ (BPDE) from the CAS-CI value are large for the H_2 molecule with the interatomic distance R(H$\cdots$H) $\leq$ 1.5Å, this large deviation is mainly caused by the Trotter decomposition. Another reason is that the spin-singlet wave function is not well approximated by $|\Psi_1\rangle$. As is possible to visualize in part a) of Fig.7, for shorter H$\cdots$H distances, the contribution of the closed shell singlet electronic configuration to the full-CI wave function becomes significant; therefore, contributions from other electronic states to $|\Psi_1\rangle$ are not negligible [1]. As a result, the likelihood function becomes a

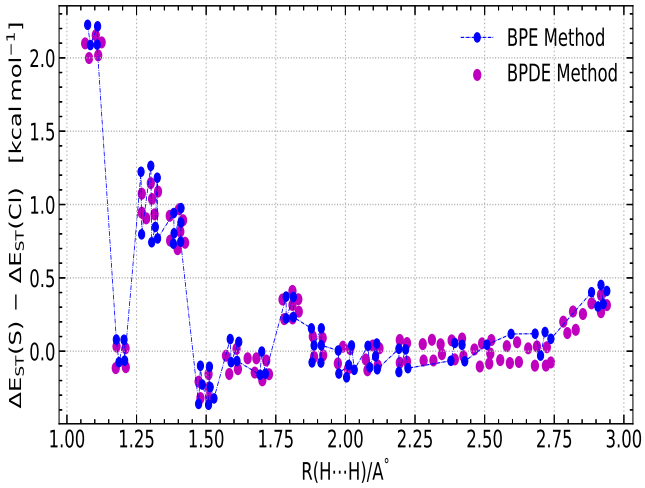

FIG. 7: Differences between the singlet–triplet energy gaps from the quantum circuit simulations and those from the CAS-CI calculations for H_2 molecule with different atom–atom distances. Adapted from [1].

—	ΔE_{S-T}/kcalmol^{-1}		
R(H…H)/Å	BPE	BPDE	Full-CI
1.2	-141.3345	-141.3351	-143.2589
1.3	-112.9313	-112.9511	-112.9205
1.4	-86.9323	-86.9099	-87.8766
1.5	-66.7065	-66.6968	-67.4980
1.6	-51.7065	-51.3740	-51.1805
1.7	-38.377	-38.3720	-38.3343
⋮	⋮	⋮	⋮
2.0	-15.0761	-15.0716	-15.1252
2.1	-10.9444	-10.9339	-10.9075
⋮	⋮	⋮	⋮
2.5	-2.7383	-2.7318	-2.7710
2.7	-1.3282	-1.3387	-1.3486
3.0	-0.4249	-0.4359	-0.4364

TABLE I: Singlet-triplet energy gaps of H_2 molecule computed by using BPE, BPDE, and full-CI methods which its difference of convergence from figure 6. Adapted from [1].

linear combination of many cosine functions, and $P(0)$ becomes flattened. They are adopting multiconfigurational wave functions constructed using diradical character $\mathcal{Y}$ for $|\Psi_1\rangle$ using the quantum circuit proposed by Takeji Takui et al. It is a promising approach to improve the $\Delta E_{\text{S-T}}$ values, which is out of the focus of this paper review.

3.3 Vertical excitation energies

Finally, the BPDE algorithm can be implemented to compute the vertical excitation energies. However, these calculation were impossible by using the BXB algorithm, although it is essential to assign electronic transitions of the UV-vis spectra theoretically.

Spin-singlet and triplet states can be computed by using the excitation operators T_{ja} given by:

$$T_{ja}(singlet) = \frac{1}{\sqrt{2}}(a^{\dagger}_{a\alpha}a_{j\alpha} + a^{\dagger}_{\alpha\beta}a_{j\beta}) \tag{23}$$

$$T_{ja}(triplet) = \frac{1}{\sqrt{2}}(a^{\dagger}_{a\alpha}a_{j\alpha} - a^{\dagger}_{\alpha\beta}a_{j\beta}) \tag{24}$$

where j and a represent occupied and unoccupied molecular orbitals in the ground state, respectively [1] .

The excitation energies obtained from BPDE and BPE quantum circuit simulations agree with the CAS-CI value within 0.1 ev errors, verifying the BPE and BPDE accuracies.

As discussed above, the number of iterations in the Bayesian optimization does not depend on the system size in BPDE. This behavior can be observed in the calculation of CBr_2 with an error of the total energy is about 0.0035 eV. However, BPE simulations need sixteen iterations to achieve convergence.

Using tighter initial variance can accelerate the Bayesian optimization. On the other hand, the BPDE simulation demonstrates its efficiency by achieving convergence after a mere eight iterations. This direct approach to calculating the energy gap proves to be advantageous in terms of reducing the computational costs associated with Bayesian optimizations.

CONCLUSIONS

This review examined the Bayesian phase difference estimation (BPDE) algorithm. It is a general quantum algorithm that can compute the difference between two eigenphases of unitary operators, in some cases, of direct calculations of energy gaps, including vertical ionization energies, singlet-triplet energy gaps, and vertical excitation energies. The BPDE algorithm is free from the controlled-time evolution operation necessary for other algorithms, such as QPE. Also, the number of qubits required for its implementation is equal to the IQPE and BPE algorithms. The BPDE algorithm is easier to implement on quantum computers thanks to one of the most important advantages of the BPDE algorithm against the conventional BPE: the number of iterations in the Bayesian optimization to achieve convergence does not depend on the system size. However, it increases in BPE when the magnitude of the total energy becomes large[1].

The design of the BPDE algorithm is to reduce the computational cost of Bayesian optimization. Furthermore, using the BPDE algorithm is not limited

to quantum chemical calculations. It can be applied to other unitary operators, and other applications can be expected. Importantly, it has a variety of possible applications, such as core ionisations, core excitations, Rydberg excitations, and others. Connection of the BPDE algorithm to the sophisticated methods for the wave function preparation, such as multiconfigurational wave function preparations using diradical characters and adiabatic state preparation ASP is another important application of the algorithm as is summarised as an example of a technique of mapping also. This variety of applications makes us expect that there exists an important road to apply quantum computers to solve complex chemistry problems.

ACKNOWLEDGEMENTS

This review was supported mainly by the recent research in open access directed by Professor Takeji Takui et al. from Osaka University and the guide by Professor Duncan Mowbray in Quantum information lectures from Yachay University, Ecuador. Likewise, we thank the research groups involved in the main research, such as the JST PRESTO "Quantum Software" project, KAKENHI from JSPS, Japan, and the AOARD Scientific Project on "Molecular Spin for Quantum Technologies," USA.

REFERENCES

[1] K. Sugisaki, C. Sakai, K. Toyota, K. Sato, D. Shiomi, and T. Takui, Physical Chemistry Chemical Physics **23**, 20152 (2021).

[2] V. M. Bonillo, Universidad de La Coruña (2013).

[3] B. P. Lanyon, J. D. Whitfield, G. G. Gillett, M. E. Goggin, M. P. Almeida, I. Kassal, J. D. Biamonte, M. Mohseni, B. J. Powell, M. Barbieri, et al., Nature chemistry **2**, 106 (2010).

[4] J. Du, N. Xu, X. Peng, P. Wang, S. Wu, and D. Lu, Physical review letters **104**, 030502 (2010).

[5] M. B. Hastings, D. Wecker, B. Bauer, and M. Troyer, Quantum Inf. Comput. **15**, 1 (2014), URL https://doi.org/10.48550/arXiv.1403.1539.

[6] R. Babbush, D. W. Berry, I. D. Kivlichan, A. Y. Wei, P. J. Love, and A. Aspuru-Guzik, New Journal of Physics **18**, 033032 (2016), ISSN 1367-2630, URL http://dx.doi.org/10.1088/1367-2630/18/3/033032.

[7] R. Babbush, N. Wiebe, J. McClean, J. McClain, H. Neven, and G. K.-L. Chan, Physical Review X **8** (2018), ISSN 2160-3308, URL http://dx.doi.org/10.1103/PhysRevX.8.011044.

[8] R. Babbush, C. Gidney, D. W. Berry, N. Wiebe, J. McClean, A. Paler, A. Fowler, and H. Neven, Physical Review X **8** (2018), ISSN 2160-3308, URL http://dx.doi.org/10.1103/PhysRevX.8.041015.

[9] J. D. Whitfield, The Journal of chemical physics **139** (2013), URL https://doi.org/10.1063/1.4812566.

[10] K. Sugisaki, S. Yamamoto, S. Nakazawa, K. Toyota, K. Sato, D. Shiomi, and T. Takui, The Journal of Physical Chemistry A **120**, 6459 (2016), URL https://pubs.acs.org/doi/10.1021/acs.jpca.6b04932.

[11] K. Sugisaki, S. Yamamoto, S. Nakazawa, K. Toyota, K. Sato, D. Shiomi, and T. Takui, Chemical Physics Letters **737**, 100002 (2019), ISSN 0009-2614, URL https://www.sciencedirect.com/science/article/pii/S2590141918300023.

[12] K. Sugisaki, S. Nakazawa, K. Toyota, K. Sato, D. Shiomi, and T. Takui, Phys. Chem. Chem. Phys. **21**, 15356 (2019), URL http://dx.doi.org/10.1039/C9CP02546D.

[13] K. Sugisaki, K. Toyota, K. Sato, D. Shiomi, and T. Takui, Phys. Chem. Chem. Phys. **22**, 20990 (2020), URL http://dx.doi.org/10.1039/D0CP03745A.

[14] K. Setia, R. Chen, J. E. Rice, A. Mezzacapo, M. Pistoia, and J. D. Whitfield, Journal of Chemical Theory and Computation **16**, 6091–6097 (2020), ISSN 1549-9626, URL http://dx.doi.org/10.1021/acs.jctc.0c00113.

[15] P. J. O'Malley, R. Babbush, I. D. Kivlichan, J. Romero, J. R. McClean, R. Barends, J. Kelly, P. Roushan, A. Tranter, N. Ding, et al., Physical Review X **6**, 031007 (2016).

[16] Y. Wang, F. Dolde, J. Biamonte, R. Babbush, V. Bergholm, S. Yang, I. Jakobi, P. Neumann, A. Aspuru-Guzik, J. D. Whitfield, et al., ACS nano **9**, 7769 (2015).

[17] N. Wiebe and C. Granade, Physical review letters **117**, 010503 (2016).

[18] S. Paesani, A. A. Gentile, R. Santagati, J. Wang, N. Wiebe, D. P. Tew, J. L. O'Brien, and M. G. Thompson, Physical review letters **118**, 100503 (2017).

[19] Y. Cao, J. Romero, and A. Aspuru-Guzik, IBM Journal of Research and Development **62**, 6:1 (2018).

[20] M. Gong, S. Wang, C. Zha, M.-C. Chen, H.-L. Huang, Y. Wu, Q. Zhu, Y. Zhao, S. Li, S. Guo, et al., Science **372**, 948 (2021).

[21] A. Ahmed, A. Arvind, C. Hu, G. Johnson, M. Keyes, S. Kobla, A. Magdum, T. Mohan, B. Testa, B. Vasseur, et al. (2021).

[22] K. Sugisaki, K. Toyota, K. Sato, D. Shiomi, and T. Takui, Chemical science **12**, 2121 (2021).

[23] R. Orus, S. Mugel, and E. Lizaso, Reviews in Physics **4**, 100028 (2019).

[24] K. Sugisaki, C. Sakai, K. Toyota, K. Sato, D. Shiomi, and T. Takui, The Journal of Physical Chemistry Letters **12**, 11085 (2021).

[25] K. Bharti, A. Cervera-Lierta, T. H. Kyaw, T. Haug, S. Alperin-Lea, A. Anand, M. Degroote, H. Heimonen, J. S. Kottmann, T. Menke, et al., arXiv preprint arXiv:2101.08448 (2021).

[26] Y. Matsuzaki, H. Hakoshima, K. Sugisaki, Y. Seki, and S. Kawabata, Japanese Journal of Applied Physics **60**, SBBI02 (2021).

[27] K. Sugisaki, K. Toyota, K. Sato, D. Shiomi, and T. Takui, Chem. Sci. **12**, 2121 (2021), URL http://dx.doi.org/10.1039/D0SC04847J.

[28] K. Sugisaki, K. Toyota, K. Sato, D. Shiomi, and T. Takui, The Journal of Physical Chemistry Letters **12**, 2880 (2021), pMID: 33724039, URL https://doi.org/10.

1021/acs.jpclett.1c00283.